

MDO-723-0040  
February 1, 2006  
Page 1

**SPACE REACTOR MATERIALS  
MATERIALS DEVELOPMENT ORGANIZATION**

**SPACE MATERIALS MEMORANDUM**

**TITLE:** **Comparison of Fission Product Yields and Their Impact**

**AUTHOR:** **Shay Harrison**

**ATTACHMENT:** **Fission Product Yield Calculations Using ORIGEN-S and RACER  
Computer Codes, dated February 1, 2006**

---

**Abstract**

This memorandum describes the Naval Reactors Prime Contractor Team (NRPCT) Space Nuclear Power Program (SNPP) interest in determining the expected fission product yields from a Prometheus-type reactor and assessing the impact of these species on materials found in the fuel element and balance of plant. Theoretical yield calculations using ORIGEN-S and RACER computer models are included in graphical and tabular form in Attachment, with focus on the desired fast neutron spectrum data. The known fission product interaction concerns are the corrosive attack of iron- and nickel-based alloys by volatile fission products, such as cesium, tellurium, and iodine, and the radiological transmutation of krypton-85 in the coolant to rubidium-85, a potentially corrosive agent to the coolant system metal piping.

**Background**

The performance demands on Prometheus-1 fuel elements were unique. Conventional nuclear reactor fuel elements generally operate for relatively short lifetimes (~3-6 years in commercial reactors), at relatively low temperatures, and are utilized in an environment where periodic inspection and replacement of defected fuel elements is possible. For Prometheus-1, fuel elements would have needed to operate at extremely high temperatures (up to 1450 K in some concepts) for periods of 15 or more years. Inspection and replacement would not be possible, so an extremely high degree of reliability was necessary.

Fulfilling these requirements necessitated a detailed understanding of how the various components of a fuel element interact. In particular, studies of the interaction of fuel and fission products with reactor core components (claddings, liners, springs, etc) and down stream with plant components were well underway. Due to the restructuring of the space program, the project was discontinued.

Prior to closeout, the fuel for Prometheus-1 was chosen to be UO<sub>2</sub> because it offers fewer compatibility issues than UN [1]; however, a liner/clad combination was not selected. Table 1 lists several combinations that were under consideration.

Table 1. Candidate Core Materials with Re Liner

Material System	Cladding Material
Refractory Metal Alloys	Mo-41.5 Re
	Mo-47.5 Re
	Ta-10W
	ASTAR-811C (Ta-8W-1Re-0.7Hf- 0.025C)
	FS-85 (Nb-27Ta-10W-1Zr)
Silicon Carbide	SiC

Fission product attack has been found for virtually every material under consideration. This makes component compatibility for long times at high temperature a key materials challenge for a Prometheus type reactor. This report presents estimates of fission product inventories and discusses the potential impact of these species on the system in the event of a fuel breach. A related compatibility analysis focused on selecting the fuel element system as well as proposed capsule testing [2]. A second testing effort using simulated fuel (SIMFUEL) was planned [3] SIMFUEL is a material that represents the chemical and physical nature of irradiated fuel without undergoing actual irradiation exposure. A theoretical physics study for fission product yield values was undertaken using expected prototypical parameters in order to support the SIMFUEL project [4]. The physics study provided yield data that were employed in SIMFUEL formula calculations, which are dependent on the desired atomic percent burnup level of <sup>235</sup>U that is to be represented.

### Fast Neutron Spectrum Fission Product Yields

There were several sources for fission product inventory yield values for a notional fast reactor. They include: a) RACER Monte Carlo neutron transport code calculations [4, 5], b) a GE report [6], and c) a preliminary ORIGEN-S based estimate [2]. The RACER code assumes a defined constant power for each depletion calculation time step, which results in a nearly linear relationship of the fission product inventory yields to the integrated number of fissions. Calculations of the isotope inventory from the beginning through the end of an assumed mission (1 MWT-h, 17.2 years) included the total mass of <sup>235</sup>U fissioned and masses of fission product species produced. Using these values, the atomic fraction yield for each fission product isotope was normalized to the moles of <sup>235</sup>U fissioned, assuming that two particles result from each <sup>235</sup>U atom fission event. A liquid metal reactor concept model, developed and evaluated early in the NRPCT project with uranium nitride fuel, niobium-zirconium cladding, and lithium coolant, was utilized for this isotope inventory study because it used an expanded set of fission products in the depletion calculation. The RACER calculation method is comparable to that employed by the ORIGEN-S computer code, which is also available at NRPCT facilities, except that RACER uses actual isotopic reaction rates from the Monte Carlo reactor physics simulation. ORIGEN-S can provide yields from three specified neutron energy ranges, 0.0253 eV, 500 keV, and 14 MeV with approximated one or two energy group neutron cross sections for the fission and absorption reaction rates. Figure A1 in Attachment presents the ORIGEN-S fission product cumulative yield data for the three different neutron energy levels. The 500 keV energy range was

determined to be appropriate for the neutron energy spectrum of the Prometheus reactors being considered. In essence, the thermal spectrum (0.0253 eV) and fast spectrum data are quite similar, except for the increased yields in the valley region between the two high yield mass number peaks (~95 and 140 amu). The 14 MeV energy level was deemed too high for the Prometheus reactor conceptual operating conditions. The ability to calculate non-thermal energy fission product yields is not available in the RACER model, in which the yield calculations are tied to the 0.0253 eV ORIGEN-S based yield fractions and are not dependent on the neutron spectrum of the core. The isotope species in the middle, lower yield valley of the typical fission product yield graph required the use of correction factors to the RACER yields. Because RACER data did not adequately reflect the relatively higher yields for mass numbers in the 105 to 129 range of a fast energy spectrum, multiplying factors of 1.5 to 3 were used to increase the projected yield values. These correction factors produced results that better matched the ORIGEN-S 500 keV values. Figure A2 in Attachment 1 plots the adjusted RACER data with the ORIGEN-S cumulative yields for a neutron energy of 500 keV, showing a good match of the two curves. Table A1 in Attachment 1 compiles the raw fission yield data for the various elemental isotopes examined in the RACER study.

In addition to the RACER-generated data, a spreadsheet was used to predict fast reactor fission product yields based on data from a 1979 GE document [6]. These values were normalized to the total  $^{235}\text{U}$  fissions. The two fast spectrum data sets, from RACER and GE, are compiled in Table 2 below. The data were normalized so the elemental yields (instead of isotopic yields) of the major fission products sum up to a total yield of 100%. The third set of values from ORIGEN-S only is not shown because of its preliminary nature.

The RACER effective fast spectrum yield calculations show reasonably good agreement with the General Electric data. The three most significant differences were found in the yields for molybdenum, neodymium, and zirconium, but all had large yield fractions regardless of the data source. The third data [2] set showed similar results. A preliminary analysis was performed to identify the likely sources for the differences in yields obtained from the various calculations. The three factors identified were:

1. Assumption of cross sections and yield fractions:

Both RACER and the ORIGEN calculations used the thermal energy fission product yield fractions. The RACER cross sections used were the standard continuous energy values based on the model flux spectrum. The RACER yields were adjusted in the middle mass number range to match the 500keV data. The ORIGEN calculations used an effective one group fast spectrum cross section and depleted to a higher %FIFA. The resultant effective thermal spectrum yields were not adjusted in the middle mass number range. Depending on the transmutation and decay of the fission products after they are produced, the inventory will differ due to depletion timestep size and cross sections.

2. Instantaneous evaluation of the isotope decay:

The isotopic values from the ORIGEN calculations could have been reported at an instantaneous point during burnup, or after a power down and delay during which transient isotope decays (i.e. isotopes with half-lives less than a few days) occurred. Depending on the decay time, the amount of shorter-lived relative to the longer-lived isotopes will be different as compared to the ORIGEN cumulative yields.

### 3. Unit comparison

The third data set is believed to be determined initially from units of grams of fission product/grams of  $^{235}\text{U}$  fissioned, whereas the RACER data generated for this evaluation were initially the mass inventory of each isotope at each time step of the model depletion and then converted to an atom fraction yield per atom  $^{235}\text{U}$  fissioned.

**Table 2. Comparison of Fast Neutron Spectrum Fission Product (F. P.) Yields Obtained from RACER and GE Data Sets**

Fission Product Species	RACER F.P. Yields	GE F.P. Yields	Absolute Value Difference
Kr	1.89%	1.91%	0.02%
Rb	1.89%	1.76%	0.13%
Sr	4.25%	4.47%	0.22%
Y	2.43%	2.26%	0.17%
Zr	16.39%	14.93%	1.46%
Nb	0.03%	0.00%	0.03%
Mo	9.29%	12.23%	2.94%
Tc	3.13%	2.88%	0.25%
Ru	5.89%	6.09%	0.20%
Rh	1.55%	1.64%	0.09%
Pd	1.30%	1.18%	0.12%
Aq	0.05%	0.06%	0.01%
Cd	0.11%	0.09%	0.02%
In	0.02%	0.01%	0.01%
Sn	0.20%	0.19%	0.01%
Sb	0.05%	0.04%	0.01%
Te	1.24%	1.34%	0.10%
I	0.58%	0.59%	0.01%
Xe	10.97%	10.74%	0.23%
Cs	9.40%	9.74%	0.36%
Ba	4.04%	3.28%	0.76%
La	3.29%	3.17%	0.12%
Ce	6.38%	5.89%	0.49%
Pr	2.98%	2.98%	0.00%
Nd	10.43%	9.98%	0.45%
Pm	0.25%	0.00%	0.25%
Sm	1.83%	1.94%	0.11%
Eu	0.10%	0.09%	0.01%
Gd	0.02%	0.04%	0.02%

The RACER data were ultimately utilized in determining powder mixture formulas for SIMFUEL material, based on the atomic percent burnup of  $^{235}\text{U}$ . Methodology to compute the amount of each fission product species, in grams per cubic centimeter, was included [4] based on the yields and burnup level. From this density value, a weight percent can be estimated for the appropriate oxide compound containing the desired fission product. Full SIMFUEL powder mix formulas were generated for 1, 2, 3, 4, 5 and 6  $^{235}\text{U}$  atomic percent burnups. These formulas are detailed in [3].

### Thermodynamics and Fission Products Remaining in the Fuel

Table 2 shows relatively low fission product yields of Nb, Gd, Eu and Pm. These fission product species were neglected from subsequent impact analysis.

Feasibility of chemical reactions occurring between fission products and  $\text{UO}_2$  fuel is determined by the standard free energy of formation ( $\Delta G_f$ ) of fission product oxides and temperature. To determine whether the formation of an oxide is energetically favorable, a plot of standard free energy of formation of oxides of fission products per mole of oxygen ( $\text{O}_2$ ) as a function of temperature is shown in Figure 1. In this figure, the more negative the free energy, the more stable is the oxide. To predict whether a fission product species will oxidize, the standard free energy of formation of oxide must be more negative than the free energy of formation of  $\text{UO}_2$  that is approximately 410 kJ per mole at 1500 K [7]. Conversely, if  $\Delta G_f$  is more positive than that of the  $\text{UO}_2$ , the fission product will not oxidize. The pure stable state leaves the fission products free to form inclusions or allows it to diffuse out of the fuel to the plenum.

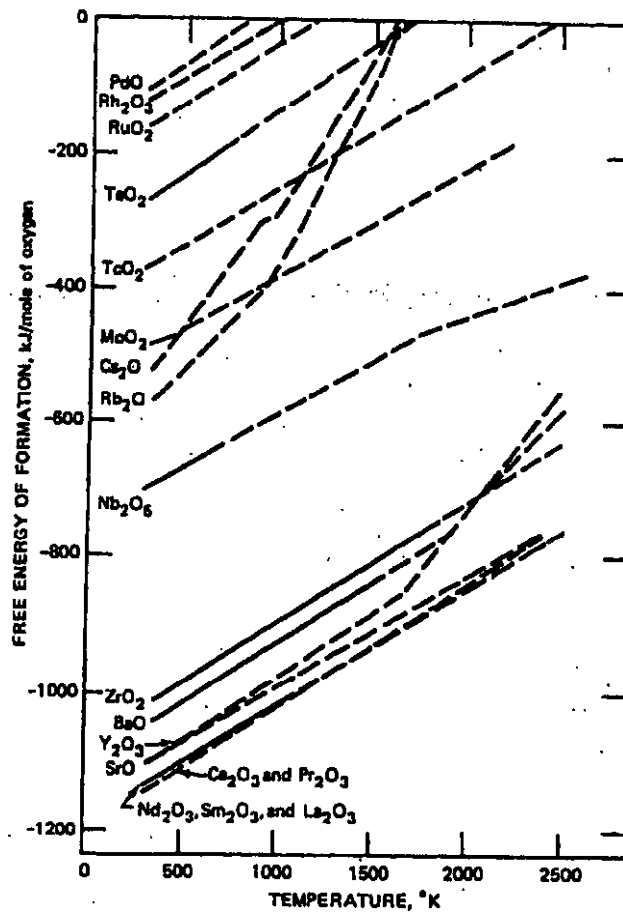


Figure 1: Free energy of formation for fission product oxide materials [7] , pg. 179)

Historically, irradiated oxide fuel samples have shown microstructural features that are consistent with thermodynamic predictions [7-14]. These studies date to the 1960's and 1970's and are repeatedly cited in subsequent literature as seminal and definitive examinations. Utilizing Figure 1, a variety of fission products would be oxidized assuming a fuel peak core temperature (PCT) of 1500 K for the Prometheus design. Rare earth oxides of lanthanum,

cerium, praseodymium, neodymium, and samarium with significantly lower formation energies are quite stable. These rare earth species in the fission product due to their multiple oxidation states will form different oxides, such as  $\text{CeO}_2$  ( $\text{Ce}^{+4}$ ) and  $\text{Ce}_2\text{O}_3$  ( $\text{Ce}^{+3}$ ). Some stable rare earth oxides, e.g., yttrium oxide, are soluble in  $\text{UO}_2$ . The alkaline earths, barium and strontium, also form stable oxide compounds, though the oxides are not soluble in the  $\text{UO}_2$  matrix due to the large ionic radii of the  $\text{Ba}^{2+}$  and  $\text{Sr}^{2+}$  ions. Zirconium oxide forms a solid solution with  $\text{UO}_2$ ; however, not all zirconium produced from fissioning will react to yield  $\text{ZrO}_2$ . The free Zr remaining will typically interact with the alkaline earth oxides to form zirconates,  $\text{BaZrO}_3$  and  $\text{SrZrO}_3$ . These zirconates have a perovskite crystal structure. They appear as island precipitates called the grey phase based on microscopic observations. Cerium has also been found in the zirconate formation because it is the stable end isotope of the mass 140 decay chain that includes  $^{140}\text{Ba}$ .

Several transition metal fission product oxides are thermodynamically unstable in oxide fuel, including technetium, rhodium, ruthenium, and palladium. Molybdenum oxide has a free energy of formation that is approximately the same as that of  $\text{UO}_2$ , making it more prone to local perturbations in the energy state. As a result, Mo can be found both as an oxide and as an unbound element simultaneously present in irradiated oxide fuel. Mo, Ru, Tc, Pd, and Rh have been shown to react together and form insoluble intermetallic inclusions in the fuel matrix, thus reducing the mobility of these fission products. These intermetallic compounds are referred to as white inclusions. Mo is believed to control the oxidation state in a manner equivalent to a buffer in aqueous solutions, preventing large swings in the oxide fuel oxygen potential by shifting from elemental  $\text{Mo}^0$  to  $\text{MoO}_2$  ( $\text{Mo}^{+4}$ ). Calculations with modern thermodynamic databases that include mixed-oxide compounds suggest that  $\text{MoO}_2$  will react with alkali metal oxides, based on the reaction:  $2 \text{Cs}_2\text{O} + 3 \text{MoO}_2 = \text{Mo} + 2 \text{Cs}_2\text{MoO}_4$ . This, however, does not change the conclusion that Mo will exist in at least two different oxidation states, and act as an "oxygen buffer".

There is uncertainty concerning the behavior of Pd and other period 5 fission product metals. Not all of the Pd may react and be accounted for in the intermetallic phases, leaving some available to diffuse out of the fuel and interact with components of the surrounding fuel element. The other period 5 metals that are found in very limited amounts, silver, cadmium, indium, tin, and antimony, have been shown to be part of the different intermetallic phases; however, there is evidence of various Pd-In-Ag-Cd-Sn precipitates that have escaped their fuel form and deposited in the open fuel-clad plenum volume [15]. In considering Ag, Cd, In, Sn, and Sb, Table 2 indicates that these are five of the eight lowest yield species. An analysis was conducted to determine how thick a layer each fission product would coat out on the inner diameter surface of a prototypical fuel pin, presuming all of the atoms escaped from the fuel pellet. Table 3 below shows that while the amounts are rather small, the thicknesses are not a matter of one or two monolayers.

**Table 3: Calculated coat-out thicknesses for noble metals in a prototypical fuel pin**

Elemental Species	Thickness (monolayers)	Thickness (Angstroms, $10^{-8}\text{cm}$ )
In	20	27
Ag	40	48
Sb	70	95
Cd	100	132
Sn	160	225

Xenon and krypton are noble gas fission products that do not chemically interact with  $\text{UO}_2$  fuel. These gases can be found in solution with the oxide matrix, in closed inter- and intragranular bubbles, and in interconnected grain boundaries that provide escape paths to the pellet surface and fuel plenum. The Xe yield is over an order of magnitude greater than that of Kr, and therefore is the main noble gas concern. The amount of Xe released from irradiated fuel depends on the fuel density, fuel temperature, and burnup level. Intuitively, a decrease in density provides more gas release paths, leading to increased gas release. Likewise, increasing the fuel temperature and burnup produces higher gas release from the fuel. The total gas release (the vast majority of which would be Xe) from a fuel form in a Prometheus-type reactor was predicted to be in the 50 to 85% range (Reference 16). The amount of gas release has a strong dependence on the fuel matrix grain size. Approximately 100% gas release was considered to be a real possibility over the long life of a Prometheus fuel system.

Cesium, rubidium, iodine, and tellurium are volatiles at Prometheus-type fuel operating temperatures, indicating that these species will likely escape from a fuel pellet. Based on thermodynamic modeling, a significant amount of Cs reacts with Mo and O to form cesium molybdate,  $\text{Cs}_2\text{MoO}_4$ . Cesium molybdate is another volatile that enables the escape of both cesium and molybdenum to the fuel plenum volume, which has been verified experimentally (References 13-14). Iodine has been reported to have a high diffusion coefficient in irradiated  $\text{UO}_2$ , almost 100X greater than xenon, and showed significant release from irradiated fuel samples [17].

A potentially useful fuel element engineering feature is shown in Figure 1 concerning the thermodynamic properties of rubidium and cesium. At elevated, operating fuel temperatures like the notional Prometheus PCT,  $\text{Rb}_2\text{O}$  and  $\text{Cs}_2\text{O}$  are not energetically favorable to form in oxide fuel. However, at temperatures below approximately 600 K, both oxide species would be predicted to form. This behavior could be utilized in fuel element design to capture volatile Rb and Cs that escape the oxide fuel by condensing the species out at the 'cold' ends of the fuel pin. This fuel pin 'cold finger' condensation process was demonstrated in UN fuel during the SP-100 program, forming elemental Cs at the pin ends [18, 19]. In a  $\text{UO}_2$  fuel system, the Rb and Cs atoms, once condensed out on the cooler oxide fuel surface, could be energetically favored to form their respective oxides presuming available oxygen. This process would bind these volatiles and prevent them from attacking the other fuel element components.

The preceding chemical interactions and microstructural formations bind up the majority of species produced from the fissioning process. The materials that remain, except for the noble metals, are gaseous and volatile in nature: (noble gases) xenon, krypton, (volatiles) iodine, rubidium, cesium, and tellurium.

### Consideration of Fission Products in Uranium Nitride

Uranium nitride has a markedly different behavior with fission products compared to  $\text{UO}_2$ . Thermodynamics predicts very few, if any, fission product binary nitrides to form, and there is little experimental evidence to contradict this theory. The noble gases and volatiles presumably escape the fuel via the same processes at work in  $\text{UO}_2$ . The rare earths, such as Ce and La, are believed to form soluble nitrides in the fuel matrix. The interaction of the transition metals with UN poses the most deleterious consequence for the fuel element. UN has been shown to be chemically attacked by Ru, Pd, Mo, Rh, and Tc, with Ru being the most predominant metal fission product species found in irradiated UN (References 20-21). U-metal compounds, i.e.  $\text{URu}$ ,  $\text{URh}$ , etc, typically have significantly lower melting points than the UN fuel and consequently create free-flowing liquids in the fuel body. These liquid compounds were shown

to chemically attack and degrade surrounding clad layers. As part of the fission product dissociation of UN, Zr is believed to tie up nitrogen freed by the chemical attack of uranium.

### **Fission Product Interactions External to the Fuel Form**

Little information in the literature was found on fission product interactions with refractory metals and their associated alloys, such as tungsten, rhenium, tantalum, and molybdenum-based materials. This is an area that would have required both experimental and theoretical investigation to assure performance is not compromised by fission product chemical attack.

#### **Cesium and Tellurium Interactions**

Cs and Te are volatiles that have revealed corrosive impact upon potential clad/liner and structural materials after escaping the fuel. Both have shown, when present at high concentration, significant attack on iron-nickel based alloys during material couple testing [22-26]. Stainless steels, such as 304 and 316 are corroded by Cs. To combat the corrosive attack of Cs, the O<sub>2</sub> potential must be such that the Cs oxide is stable. Without meeting this oxygen prerequisite, Cs was compatible for 3000 hours at 1000°C in one study. Cs typically targets Cr during intergranular corrosion, leaving CrO<sub>3</sub> and Cs<sub>2</sub>CrO<sub>4</sub> deposits. Te by itself, or as the oxide TeO<sub>2</sub>, shows similar, damaging behavior. The presence of Cs and Te together is more appropriate to conditions in a fuel element. Differing ratios of Cs:Te exposed to steel for over 150 hours at 675°C reveal two corrosive attack modes. One is intergranular (IG), while the other is matrix corrosion, a layered type oxidation that creates alternating Cr-rich and Fe-rich layers. The mixture of IG and matrix corrosion for Cs:Te ratios was seen in several investigations. Post-test materials characterization showed formations of Cs<sub>2</sub>CrO<sub>4</sub>, CsFeO<sub>2</sub>, and FeTe corrosion product compounds. Without oxygen present, the Cs:Te combination was inert to austenitic stainless steels.

Silicon carbide has been used in TRISO-type, layered fuel particles in high temperature gas reactor (HTGR) applications as a barrier to Cs escape from the particle. Cs has a low diffusion coefficient in SiC, with dependence of D<sub>eff</sub> on SiC deposition conditions and the resulting microstructure (Reference 29). If the SiC coating cracks and fails, Cs can find open pathways to escape the particle. Ceramic additives to coating layer precursor mixture, such as alumina and silica, served to augment the diffusion barrier effect at fuel temperature below 1200°C (1473 K, approximately the proposed Prometheus-type reactor fuel peak core temperature) for Cs transport (Reference 30).

#### **Rubidium Interactions**

Rb is produced from uranium fissioning on the order of 1/5 the amount of Cs. It is directly above Cs in the alkali group on the periodic table and exhibits similar chemical behavior. Due to its lower quantity, however, Rb has garnered significantly less concerns for compatibility with candidate fuel element materials. The one situation that has merited scientific attention is the containment and storage of the radioactive isotope <sup>85</sup>Kr. Krypton-85 undergoes radioactive decay to form <sup>85</sup>Rb (see Radiological Concerns discussion below), and therefore corrosive attack by Rb on potential container materials was investigated [31-32]. A variety of stainless steels, chromium-molybdenum steels, and nickel-based alloys have been studied, as well as material interactions in the Rb-Cr-O system. Liquid chromium was found to getter oxygen from rubidium oxide at low oxygen potentials to likely form RbCrO<sub>2</sub>, while at higher oxygen potentials, an Rb<sub>4</sub>CrO<sub>4</sub> compound was produced. 316 stainless steel was minimally affected by exposure to liquid Rb, while a liquid Rb-5 wt.% O solution resulted in noticeable corrosive attack. In other

work, 304 stainless, A286/AISI 660 (another stainless alloy), and AISI 4130 (chromium-molybdenum, low carbon steel) were eliminated as possible container materials due to their susceptibility to corrosion.

### Xenon and Krypton Considerations

By nature, inert gases, Xe and Kr, will not chemically interact with fuel element or plant materials with which they come in contact. These gases likely escape through the fuel element and enter the cooling system. Their impact on the heat transfer properties of the coolant was the main consideration. The effect on coolant thermal conductivity by fission product Xe and Kr gas additions was evaluated [33]. In this study, the coolant was assumed to 78% helium and 22% Xe. Pin rupture was assumed to be the failure mode, thereby releasing all Xe and Kr as well as Rb and Cs that condensed in colder regions of the fuel pin. The study concluded that the impact on the heat transfer coefficient would be minor, likely insignificant compared to uncertainties in the heat transfer correlations. As such, future space nuclear power research efforts can focus on examining other fission product species and presume Xe and Kr will not produce deleterious effects, other than potential gas pressure buildup in a sealed fuel element.

### **Radiological Concerns**

There are two fission product isotopes that have radiological considerations pertinent to the Prometheus-1 project,  $^{85}\text{Kr}$  and  $^{137}\text{Cs}$ . Both isotopes are expected to escape the fuel pellet. Krypton, as an inert gas, will likely permeate the fuel element and enter the coolant stream.  $^{85}\text{Kr}$  was predicted to be approximately 4.8% of the total krypton fission product yield, with a half life of 10.76 years. This species undergoes beta decay to form rubidium-85,  $^{85}\text{Rb}$ , which acts as a reactive volatile.  $^{85}\text{Rb}$ , although in a limited available amount, could attack iron and nickel-based coolant and plant components. Cesium is a reactive volatile as well and is expected to be free in the fuel plenum volume to interact with fuel element materials.  $^{137}\text{Cs}$  was calculated to be approximately 27.9% of the total cesium fission product yield, with a half life of 30.07 years.  $^{137}\text{Cs}$  transmutes via beta decay into  $^{137}\text{Ba}$ . Barium is a significantly less reactive species than cesium and will likely bind to oxygen and form an oxide, thus removing a small amount of the cesium from the fuel element system. In addition, Kr and Cs isotopes generate high energy gamma radiation during their respective decay processes.  $^{85}\text{Kr}$  emits 151.2 keV gamma radiation, while  $^{135}\text{Cs}$  and  $^{137}\text{Cs}$  both produce gamma rays at 787.2 and 661.7 keV energies, respectively. These gammas have the potential to lead to ionization damage in the plant systems after the shield. Of particular concern in the plant design was potential irradiation damage from radioactive species in the coolant to the electrically insulating polymeric materials in the alternator. Degradation of these polymer insulators could lead to a catastrophic short circuit in the alternator. To protect the alternator, which supplies power for the scientific instrument package and other systems, a condensation trap in colder sections of the coolant circuit could be implemented in the design to isolate the radioactive Cs.

### Iodine Interactions

Iodine has been studied extensively in the last 30+ years by the nuclear scientific community due to its propensity to cause stress corrosion cracking (SCC) in a variety of zircaloy clad materials. Iodine attack leads to embrittlement of zircaloy layers. This focus, unfortunately, has precluded basically any investigation into other materials that would be candidate fuel element layers. Stainless steel has been shown, in non-nuclear oriented studies, to corrode in iodine environments, but review of the open literature indicates that this is the limit of research in the field.

Thermodynamic and experimental evidence indicates that Cs and I will react to form CsI in the fuel and plenum, but the extent of reaction is not resolved. This molecule is thermodynamically predicted to be very stable, but has been shown to corrosively attack stainless steels in hyperstoichiometric UO<sub>2</sub> (Reference 23). The iodine corrosion mechanism may arise from free iodine or from disassociation of the CsI molecule by radiation. Ta, Mo, and Nb may be susceptible to the same iodine embrittlement found with Zircaloy materials, but this will need to be experimentally verified. SiC, as a layer on sealed, coated TRISO fuel particles, has been shown to be an effective diffusion barrier to iodine (Reference 34).

Pd, Ag, Cd, In, Sb (Period 5 noble metals)

The noble metal elements are not expected to form chemical compounds with the oxygen available in irradiated uranium oxide fuel. While they may form intermetallic compounds or solution phases with other fission products, or with uranium, these compounds and phases are not sufficiently stable to completely suppress their volatility. Adding other substances to the fuel to "getter" these elements by forming compounds with them is unlikely to be successful for the same reason, because all of their compounds decompose to a significant extent at high temperatures. Palladium has the highest fission yield of this group, but the others have lower boiling points (see Table 4 below). Given the high boiling point of palladium, it seems surprising that it would act as a volatile element in fission product mixtures, but there is evidence that Pd migrates as a volatile species [35-36]. Fission product palladium has been found to attack silicon carbide in developmental HTGR fuel (Reference 37). Palladium interacts particularly strongly with silicon, forming high-melting compounds and very deep eutectics (liquid solutions with lower freezing points than the individual elements). Use of sacrificial silicon carbide layers in the fuel appears to be one of the most promising approaches to manage palladium attack in ceramic-clad fuels [38]. The other noble metal elements have not been observed to attack silicon carbide, but silver has been observed to diffuse through SiC and graphite with surprising ease [39].

Little is known about how these noble metals interact with refractory metal alloy cladding. The most likely form of attack is embrittlement, but not much is known yet about embrittlement of refractory metal alloys by volatile fission products. There is no reliable way to predict from theory which low-melting metals may embrittle which refractory metals. In SP-100 irradiation tests with UN, tungsten liners often cracked. The cracking was attributed to fission product embrittlement, but follow-up experiments to identify the responsible fission product(s) were not performed. Rhenium liners appeared to be resistant to cracking in similar tests.

Experimental testing in the SP-100 program revealed copper contamination, originating from the manufacturing process, that was found in conjunction with embrittlement of Nb-1Zr and Re materials. Nb-1Zr specimens contaminated with copper or copper alloys suffered brittle intergranular fracture. Nb-1Zr specimens contaminated with cadmium, silver, or tin showed slight to moderate reduction in uniform elongation, but still failed in a ductile manner. Palladium was not tested. In one set of tests, ductile failure with slight to moderate reduction in elongation was observed for nickel and platinum contamination, which are directly above and below Pd, respectively, on the periodic table (and have lower and higher-melting temperatures, respectively, than Pd). In an earlier set of tests, though, Nb-1Zr specimens contaminated with nickel and platinum showed 50% degradation of ductility [40].

Embrittlement of titanium alloys by cadmium has been observed [41-42]. The literature appears to contain few if any reports on embrittlement of molybdenum, rhenium, or Mo-Re alloys by any of these noble metal elements, but the SP-100 experience with tungsten liners suggests that

embrittlement of Mo may be possible, because Mo is directly above tungsten on the periodic table.

**Table 4. Noble Metal Physical Properties**

Property	Pd	Ag	Cd	In	Sn
U235 fast fission yield of isotopes (based on 2 fission product atoms per U atom fission event)	2.60	0.10	0.22	0.04	0.40
melting point, K	1825	1235	594	387	505
boiling point, K	3234	2432	1039	458	2873
vapor pressure of pure element at 1500 K, bars	1.9E-7	3.6E-4	>1	>1	1.1E-5

### **Commercial High Temperature Gas Reactor (HTGR) Experience**

Examination of fission products interactions with plant materials in functional gas reactors has been very limited in the commercial arena. The reason for this lack of interest by commercial operators is succinctly stated by K.H. Dent in a general overview article about gas-cooled reactor technologies and performance, "Under normal operating conditions all but less than 1% of the fission products are retained in the uranium dioxide fuel lattice [43]. Analysis of fuel pin failures in Advanced Gas Reactors (AGRs) in Britain revealed little release of fission products. Pin failures in Hinkley Point B and Hunterston B reactors showed very low (effectively zero) leak rates and little effect on the coolant activity (Reference 44). High tortuosity escape paths lead to small amounts of only noble gases releasing to the coolant. A significant amount of research has been conducted on the plateout behavior of species like  $^{137}\text{Cs}$ ,  $^{90}\text{Sr}$ ,  $^{131}\text{I}$ , and  $^{110\text{m}}\text{Ag}$  in reactor loop tests. The testing evaluated the amount of surface activity, i.e. Curies/cm<sup>2</sup>, of a particular fission product species that had been deposited on a sample tube in the loop. Test facilities included in-pile loops like VAMPYR-I and -II in the AVR (German) reactor, Dragon HTGR in Britain, and Oarai Gas Loop #1 in the Japan Materials Testing Reactor (JMTR), as well as out-of-pile loops such as the HRB LAMINAR loop and General Atomics' deposition loop [45]. The deposition of Cs and I was measured in the primary coolant circuit. These species were found to preferentially plateout in evaporator/economizer sections of the steam generator, two of the colder locations in the circuit [46]. Presumably in a space reactor design, similar condensation behavior for escaped volatile fission product species would occur in the coolant. The most important lesson from commercial HTGR experience is the fact that corrosive and radiological interactions of fission products in the coolant circulator system did not lead to failures in system components. Performance reviews of the AVR Julich reactor in Germany (over 20 years) and the Fort Saint Vrain reactor in Colorado (over 10 years) did not indicate any deleterious effects on the helium circulator system by fission products that had escaped the fuel containment barriers and become entrained or plated-out in the coolant pathways [47-48].

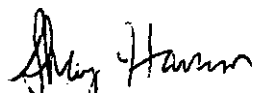
## Conclusions and Recommendations

The selection of UO<sub>2</sub> as the fuel for a space reactor greatly simplifies the challenges in dealing with free fission products, in comparison to those associated with UN fuel. A majority of the species is tied up in UO<sub>2</sub> as soluble binary oxides, insoluble ternary oxides, or intermetallic precipitates. Of the remaining fission products, many are very likely to escape the fuel form and interact with materials in the fuel element and coolant system. The preponderance of experimental investigation into these interactions over the past 40 years has been with iron- and nickel-based alloys. There are many unanswered questions about corrosive attack and embrittlement by volatiles (I, Cs, Rb, Te), in combination or singularly, on refractory metal alloys and high temperature ceramics. Future research on fission product compatibility for a nuclear-powered space reactor should focus on likely candidate fuel element clad and liner (if necessary) materials and their interactions with these volatiles at application appropriate concentrations (i.e. not pure liquid exposure to a material test coupon). Simulated fuel specimens could facilitate such studies. The main compatibility issue beyond the fuel element is the radioactive decay of <sup>85</sup>Kr in the coolant system to <sup>85</sup>Rb, which corrosively attacks iron- and nickel-based alloys. Future testing will need to analyze this corrosion reaction at low Rb concentrations, and selection of material for the coolant system piping will need to include this consideration.

## Acknowledgements

The author would like to thank Tom Angelu and Amitava Guha for reviewing the report.

## Prepared by:



Shay Harrison, Materials Engineer  
Space Materials, Space Fuel Analysis and Development  
Materials Development Operation

## Approved by:



Lynne E. Kolaya, Manager  
Space Fuel Analysis and Development  
MDO, Space Materials

## REFERENCES

1. B-SE(RE)-0001, Attachment B, "Materials and Manufacturing Aspect of the Prometheus Reactor Fuel Type Selection", July, 2005
2. B-MT(SRME)-55, "Fuel System Compatibility Issues for Prometheus-1", December, 2005
3. MDO-723-0029, "Use of SIMFUEL for Enhanced Testing of Space Fuels", December, 2005
4. SPE-SRE-0015, "Fission Product Yield Information for SIMFUEL Fabrication at LLNL", September, 2005
5. "The Physical Models and Statistical Procedures Used in the RACER Monte Carlo Code" by Sutton, Brown, Bischoff, MacMillan, Ellis, Ward, Ballinger, Kelly, Schindler, Knolls Atomic Power Laboratory, July, 1999, document # KAPL-4840 (DOE/TIC-4500-R75)
6. "Compilation of Fission Product Yields", General Electric Vallecitos Nuclear Center, document # NEDO-12154-3(B), 1980, by B.F. Rider
7. DR Olander, Fundamental Aspects of Nuclear Reactor Fuel Elements, National Technical Information Service, 1976
8. "Electron Probe Micro-Analysis of Irradiated UO<sub>2</sub>", *Journal of Nuclear Materials*, Vol. 17, 1965, pp 227-236 , by Bradbury, Demant, Marti, and Poole
9. "Metallic Fission-Product Inclusions in Irradiated Oxide Fuels", *Journal of Nuclear Materials*, Vol. 25, 1968, pp 201-215 , by Bramman, Shamble, Thom, and Yates
10. "Transmission Electron Microscopy of Irradiated UO<sub>2</sub> Fuel Pellets", *Journal of Nuclear Materials*, Vol. 27, 1968, pp 216-224 , by A.J. Manley
11. "Solid Fission Product Behavior in Uranium-Plutonium Oxide Fuel Irradiated in a Fast Neutron Flux", *Journal of Nuclear Materials*, Vol. 29, 1969, pp 27-42, by O'Boyle, Brown, and Sanecki
12. "Analysis of Fission Product Ingots Formed in Uranium-Plutonium Oxide Irradiated in EBR-II", *Journal of Nuclear Materials*, Vol. 35, 1970, pp 257-266, by O'Boyle, Brown, and Dwight
13. "The Chemical Effects of Composition Changes in Irradiated Oxide Fuel Materials", *Journal of Nuclear Materials*, Vol. 41, 1971, pp 143-155, by Davies and Ewart
14. "The Chemical Effects of Composition Changes in Irradiated Oxide Fuel Materials II- Fission Product Segregation and Chemical Equilibria", *Journal of Nuclear Materials*, Vol. 61, 1976, pp 254-270, Ewart, Tayler, Horspool, and James

15. "The Chemical State of Fission Products in Oxide Fuels", *Journal of Nuclear Materials*, Vol. 131, 1985, pp 221-246, by H. Kleykamp
16. MDO-723-0027/B-MT(SRME)-34, "Attachment A: Fuel Material Properties and Guidance to Support Pre-Conceptual Design Efforts", July, 2005
17. "The Diffusion Coefficients of Gaseous and Volatile Species During the Irradiation of Uranium Dioxide", *Journal of Nuclear Materials*, Vol. 107, 1982, pp 168-184, by Turnbull, Friskney, Findlay, Johnson, and Walter
18. "Post-Irradiation Data from the SP-1 Test at 3 Atom Percent Burnup", *LANL Report WHC-SP-1050*, Los Alamos National Laboratory, 1993, by Markenas, Hales, and Karnesky
19. "Post-Irradiation Data of the SP-3R Test", *LANL Report WHC-SP-1052*, Los Alamos National Laboratory, 1993, by BJ Markenas
20. "Ceramic Fuel Development for Space Reactors", *American Ceramic Society Bulletin*, Vol. 71, 1992, pp 96-101, by R.B. Matthews
21. "Liquid Formation in Fuel Pins During Reactor Tests", *LANL memorandum # 03062*, 1987, by R.B. Matthews
22. "Grain-Boundary Penetration of Austenitic Stainless Steels by Cesium Oxide", *Journal of Nuclear Materials*, Vol. 44, pp 96-98, by Maiya and Busch
23. "Chemical Interaction of Fission Products with Stainless Steel Claddings", *IAEA-PL-463/14*, pp 237-255, by Hofmann and Gotzmann
24. "Out-of-pile Investigations of Fission Product-Cladding Reactions in Fast Reactor Fuel Pins", *IAEA-PL-463/16*, pp 269-285, by Aitken, Evans, and Rubin
25. "Grain-Boundary Penetration of Type 316 Stainless Steel Exposed to Cesium or Cesium and Tellurium", *Metallurgical Transactions A*, Vol. 6A, 1975, pp 409-415, by Maiya and Busch
26. RJ Pulham, MW Richards, and JW Hobbs, "Caesium and Its Mixtures: Their Chemical Reactions With Alloys of Transition Metals Used to Clad Reactor Fuels", chapter in Liquid Metal Systems: Material Behavior and Physical Chemistry in Liquid Metal Systems, edited by HU Borgstedt, 1995, pp 251-260
27. RJ Pulham, MW Richards, and J Edwards, "Reactions Between Caesium/Tellurium Mixtures and Advanced Clad Alloys Under a Constant Pressure of Oxygen", from Proceedings of the Conference Held on Materials for Nuclear Reactor Core Applications, 1987
28. "The Interaction of Liquid Tellurium and Tellurium Oxide With Stainless Steels", *Transactions of the Indian Institute of Metals*, Vol. 39, 1986, pp 137-146, by Khanna and Gnanamoorthy

29. "Cesium Solubility, Diffusion, and Permeation in Zirconium Carbide", *Journal of Nuclear Materials*, Vol. 73, 1978, pp 169-179, by W.A. Stark
30. "Metallic Fission Product Retention of Coated Particles with Ceramic Kernel Additives", *Nuclear Technology*, Vol. 35, 1977, pp 548-556, by Forthmann, Grubmeier, and Stover
31. "Compound Formation in the Rubidium-Chromium-Oxygen System", *Journal of Nuclear Materials*, Vol. 119, 1983, pp 154-161, by Gadd and Borgstedt
32. "Effects of Stagnant Liquid Rubidium and the Rb-5 wt% O System on a Stainless Steel at 473K", *Journal of Nuclear Materials*, Vol. 148, 1987, pp 230-234, by Suzuki, Ohno, Masuda, Nakanishi, and Matsui
33. SPP-SRE-0028, "Effect of Fission Gas Release on Coolant Conductivity in Gas Cooled Reactor for Space Applications", January, 2006
34. "Verification of Fission Product Release Model from High Temperature Engineering Test Reactor Fuel", *Journal of Nuclear Science and Technology*, Vol. 29, 1992, pp 842-850, by Sawa, Shiozawa, Fukuda, and Ichihashi
35. "Migration Behavior of Palladium in Uranium Dioxide", *Journal of Nuclear Materials*, Vol. 247, 1997, pp 50-58, by Yoneyama, Sato, Ohashi, Ogawa, Ito, and Fukuda
36. "Behavior of Metallic Fission Products in Uranium-Plutonium Mixed Oxide Fuel", *Journal of Nuclear Materials*, Vol. 273, 1999, pp 239-47, by Sato, Furuya, Arima, Idemitsu, and Yamamoto
37. "Palladium Interactions with Fission Product Barrier Materials", KAPL internal letter # CMS No. 11, 2001, by H.J. McLean
38. "Advanced Coatings for HTGR Fuel Particles Against Corrosion of SiC Layer", *Journal of Nuclear Materials*, Vol. 246, 1997, pp 215-222, by Minato, Fukuda, Ishikawa, and Mita
39. "Diffusion of Silver through Fission Product Barrier Materials", KAPL internal letter # CMS No. 10, 2001, by H.J. McLean
40. "SP-100 Materials & Fabrication Technology Lessons Learned", Martin Marietta document # YL-K8C-940008 (sequence # 1199), 1994, by P.J. Ring
41. "Embrittlement of Titanium by Liquid Cadmium", *Metallurgical Transactions*, Vol. 1, 1970, pp 2607-2613, by W.M. Robertson
42. "Solid Cadmium Embrittlement of Titanium Alloys", *Corrosion*, Vol. 26, 1970, pp 409-41, by Fager and Spurr
43. "The Standing of Gas-Cooled Reactors", *Nuclear Energy*, Vol. 19, 1980, pp 257-271, by K.H. Dent
44. "Performance of AGR fuel—Past, Present, and Future", *Nuclear Energy*, Vol. 31, 1992, pp 55-63, by Cordall, Hatton, Jackson, and Hale

45. "Fuel Performance and Fission Product Behavior in Gas Cooled Reactors", IAEA-TECDOC-978, 1997, International Atomic Energy Agency
46. "NPR-MHTGR Fuel Development Program Plan, Rev. A", EGG-NPR-8971, 1991, by McCardell, Shaber, Hobbins, Kania, Myers, Stansfield, Hanson, and Scheffel
47. "Two Decades of Excellent AGR Circulator Operating Performance at AVR Julich", IAEA document # IWGGCR-17, *Specialists' Meeting on Gas-Cooled Reactor Coolant Circulator and Blower Technology*, 1987, pp 23-30, by Ziermann and Engel
48. "Fort Saint Vrain Gas Cooled Reactor Operational Experience", NRC document # ORNL/TM-2003/223, 2003, by Copinger and Moses

**Attachment to MDO-723-0040**  
Fission Product Yield Calculations Using ORIGEN-S and RACER Computer CODES

Author: Shay Harrison

Attachment

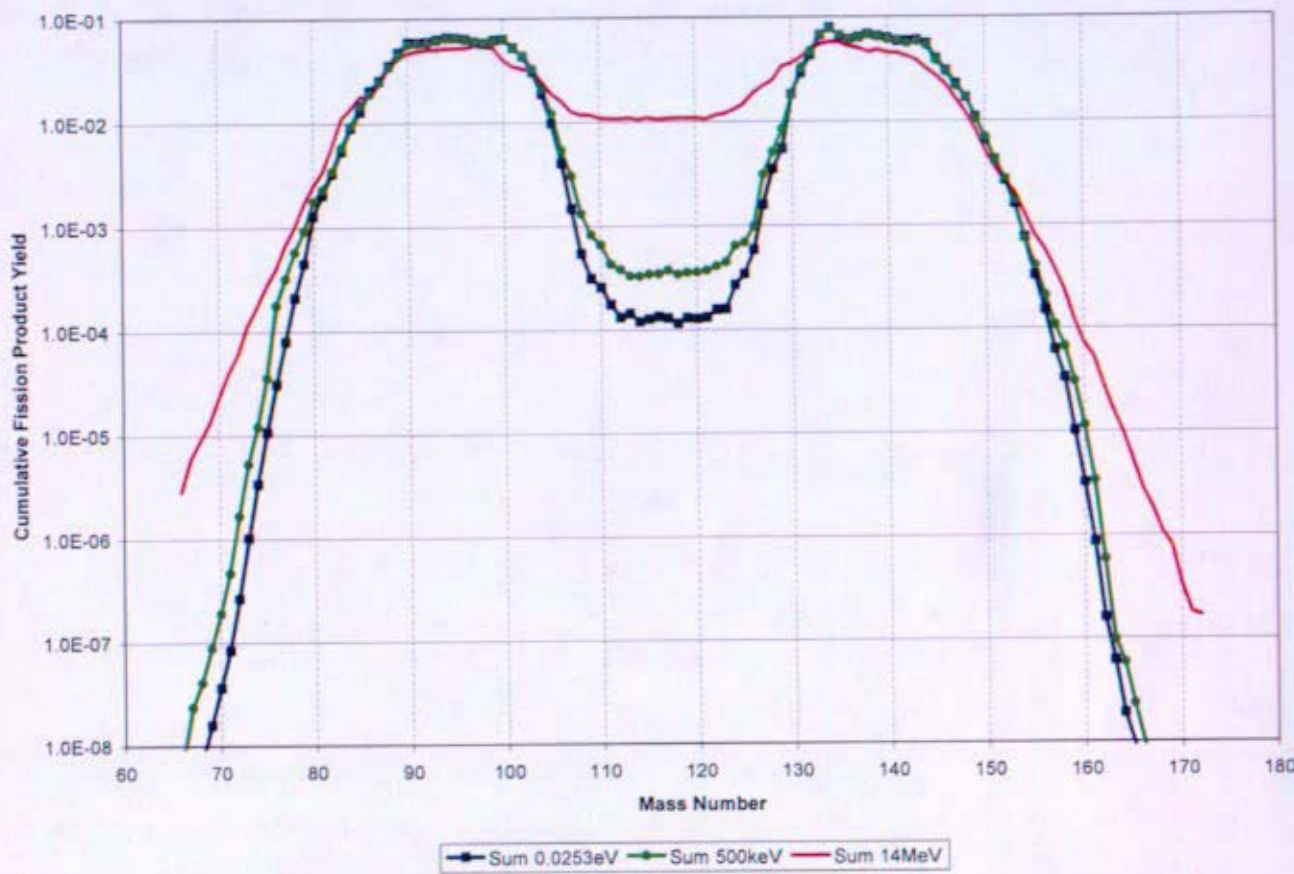
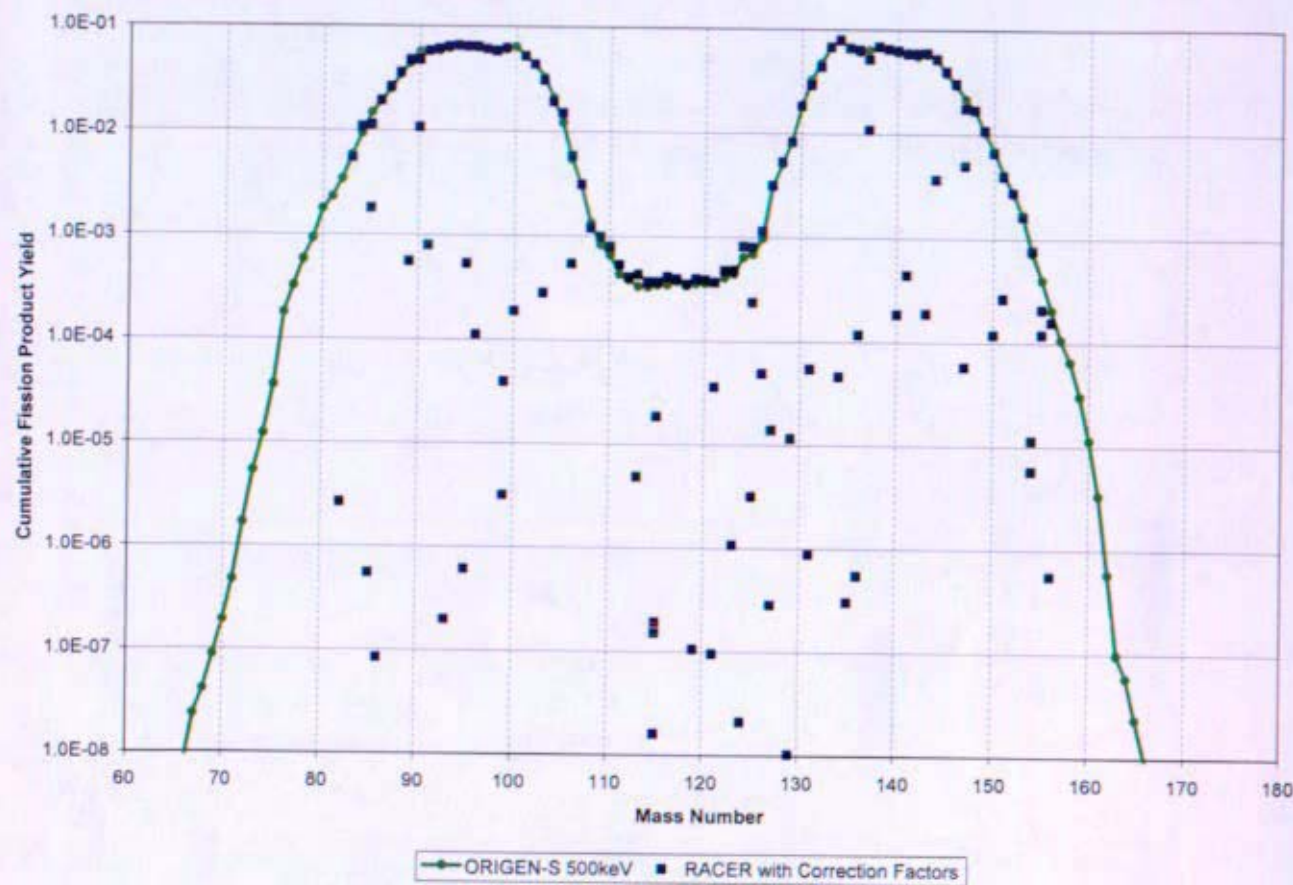


Figure A1: ORIGEN-S cumulative fission product yields for specific mass numbers from fissions with neutron energies of 0.0253 eV, 500 keV, and 14 MeV



**Figure A2:** Comparison of RACER fission product yields with correction factors applied for fast neutron energy and ORIGEN-S 500 keV cumulative fission product yield data

**Table A:** RACER computer model fission product yield data derived from the depletion masses and normalized to a total of 2.0 fission products per fission event

Isotope	Fission Product Yield	Corrected Fission Product Yield	Correction Factor
Kr-82	2.63309E-06	-----	-----
Kr-83	5.42948E-03	-----	-----
Kr-84	1.08154E-02	-----	-----
Kr-85	1.78812E-03	-----	-----
Kr-85m	5.48513E-07	-----	-----
Rb-85	1.12556E-02	-----	-----
Kr-86	1.91843E-02	-----	-----
Rb-86	8.39213E-08	-----	-----
Rb-87	2.59645E-02	-----	-----
Sr-88	3.56511E-02	-----	-----
Sr-89	5.53580E-04	-----	-----
Y-89	4.69522E-02	-----	-----
Sr-90	4.73310E-02	-----	-----
Zr-90	1.06633E-02	-----	-----
Y-91	7.92230E-04	-----	-----
Zr-91	5.79234E-02	-----	-----
Zr-92	6.05925E-02	-----	-----
Nb-93m	1.96522E-07	-----	-----
Zr-93	6.38420E-02	-----	-----
Zr-94	6.50951E-02	-----	-----
Mo-95	6.38541E-02	-----	-----
Nb-95	5.27538E-04	-----	-----
Nb-95m	6.04924E-07	-----	-----
Mo-96	1.09851E-04	-----	-----
Zr-96	6.38337E-02	-----	-----
Mo-97	6.06964E-02	-----	-----
Mo-98	5.78791E-02	-----	-----
Mo-99	3.90800E-05	-----	-----
Tc-99	6.14674E-02	-----	-----
Tc-99m	3.13443E-06	-----	-----
Ru-100	1.86888E-04	-----	-----
Ru-101	5.21220E-02	-----	-----
Ru-102	4.34103E-02	-----	-----
Rh-103	3.04028E-02	-----	-----
Ru-103	2.79039E-04	-----	-----
Ru-104	1.91036E-02	-----	-----

Isotope	Fission Product Yield	Corrected Fission Product Yield	Correction Factor
Pd-105	9.87232E-03	1.48085E-02	1.5
Pd-106	3.84288E-03	5.76433E-03	1.5
Ru-106	3.57194E-04	5.35790E-04	1.5
Ag-107	1.40763E-09	2.81525E-09	2.0
Pd-107	1.54471E-03	3.08941E-03	2.0
Pd-108	5.91192E-04	1.18238E-03	2.0
Ag-109	3.25765E-04	9.77295E-04	3.0
Pd-110	2.61621E-04	7.84862E-04	3.0
Cd-111	1.75737E-04	5.27211E-04	3.0
Cd-112	1.34189E-04	4.02566E-04	3.0
Cd-113	1.42446E-04	4.27338E-04	3.0
Cd-113m	1.60568E-06	4.81703E-06	3.0
Cd-114	1.21443E-04	3.64330E-04	3.0
Cd-115	6.34110E-08	1.90233E-07	3.0
Cd-115m	5.00609E-08	1.50183E-07	3.0
In-115	1.21329E-04	3.63987E-04	3.0
In-115m	5.32101E-09	1.59630E-08	3.0
Sn-115	6.15209E-06	1.84563E-05	3.0
Cd-116	1.35240E-04	4.05721E-04	3.0
Sn-117	1.29793E-04	3.89380E-04	3.0
Sn-117m	7.79508E-10	2.33853E-09	3.0
Sn-118	1.16348E-04	3.49043E-04	3.0
Sn-119	1.31274E-04	3.93822E-04	3.0
Sn-119m	3.50371E-08	1.05111E-07	3.0
Sn-120	1.28760E-04	3.86280E-04	3.0
Sb-121	1.20739E-04	3.62218E-04	3.0
Sn-121	3.16660E-08	9.49980E-08	3.0
Sn-121m	1.18822E-05	3.56466E-05	3.0
Sn-122	1.57750E-04	4.73250E-04	3.0
Sb-123	1.59157E-04	4.77472E-04	3.0
Sn-123	3.57544E-07	1.07263E-06	3.0
Sb-124	6.94986E-09	2.08496E-08	3.0
Sn-124	2.71099E-04	8.13298E-04	3.0
Sb-125	7.82456E-05	2.34737E-04	3.0
Te-125	2.64268E-04	7.92804E-04	3.0
Te-125m	1.04598E-06	3.13795E-06	3.0

(NOTE: Molybdenum-100 is eliminated from the fission product yields because the cross section was unavailable in RACER at the time of analysis)

Table A continued

Isotope	Fission Product Yield	Corrected Fission Product Yield	Correction Factor
Sn-126	5.67192E-04	1.13438E-03	2.0
Te-126	2.42238E-05	4.84477E-05	2.0
I-127	1.56801E-03	3.13603E-03	2.0
Te-127	1.41426E-07	2.82852E-07	2.0
Te-127m	6.95777E-06	1.39155E-05	2.0
Te-128	3.51046E-03	5.26569E-03	1.5
I-129	5.49563E-03	8.24344E-03	1.5
Te-129m	7.68886E-06	1.15333E-05	1.5
Xe-129	6.81241E-09	1.02186E-08	1.5
Te-130	1.82441E-02	-----	-----
I-131	5.40025E-05	-----	-----
Xe-131	2.90310E-02	-----	-----
Xe-131m	8.71315E-07	-----	-----
Xe-132	4.35266E-02	-----	-----
Cs-133	6.72721E-02	-----	-----
Cs-134	4.57134E-05	-----	-----
Xe-134	7.93265E-02	-----	-----
Ba-135	3.01267E-07	-----	-----
Ba-135m	8.97366E-12	-----	-----
Cs-135	6.57785E-02	-----	-----
Ba-136	1.16487E-04	-----	-----
Cs-136	5.45305E-07	-----	-----
Xe-136	6.36000E-02	-----	-----
Ba-137	1.08645E-02	-----	-----
Cs-137	5.15664E-02	-----	-----
Ba-138	6.81327E-02	-----	-----
La-139	6.46139E-02	-----	-----
Ba-140	1.84084E-04	-----	-----

Isotope	Fission Product Yield	Corrected Fission Product Yield	Correction Factor
Ce-140	6.24968E-02	-----	-----
Ce-141	4.40644E-04	-----	-----
Pr-141	5.83536E-02	-----	-----
Ce-142	5.88442E-02	-----	-----
Nd-143	5.96580E-02	-----	-----
Pr-143	1.87512E-04	-----	-----
Ce-144	3.63990E-03	-----	-----
Nd-144	5.18047E-02	-----	-----
Nd-145	3.95599E-02	-----	-----
Nd-146	3.03071E-02	-----	-----
Nd-147	5.74308E-05	-----	-----
Pm-147	4.94854E-03	-----	-----
Sm-147	1.75394E-02	-----	-----
Nd-148	1.68732E-02	-----	-----
Sm-149	1.08239E-02	-----	-----
Nd-150	6.61525E-03	-----	-----
Sm-150	1.18291E-04	-----	-----
Eu-151	2.62873E-04	-----	-----
Sm-151	3.93171E-03	-----	-----
Sm-152	2.73158E-03	-----	-----
Eu-153	1.61505E-03	-----	-----
Eu-154	1.13209E-05	-----	-----
Gd-154	5.69406E-06	-----	-----
Sm-154	7.57807E-04	-----	-----
Eu-155	1.19393E-04	-----	-----
Gd-155	2.07623E-04	-----	-----
Eu-156	5.50468E-07	-----	-----
Gd-156	1.56676E-04	-----	-----

CONCURRENCE/DESIGN CHECK FORM FOR DOCUMENT NO. MDO-723-0040 Date: 2/1/06

DOCUMENT TITLE: Comparison of fission product yields and their impact

REFERENCES B-SE(RE)-0001 SPP-SRE-0028 ENCLOSURES: (1) Fission Product Yield Calculations Using  
B-MT(SRME)-55 SPE-SRE-0015 ORIGEN-S and RACER Computer CODES  
MDO-723-0029  
MDO-723-0027/B-MT(SRME)-34

1. ADSARS: PERMANENT RECORD: Yes X No \_\_\_\_\_ Repository MFLIB Corporate Author: KAPL NR PROGRAM \_\_\_\_\_

Key Words: Fission products Fission yields UO2 Compatibility  
Need to Know Categories GEN SGN \_\_\_\_\_  
Available Sites: PRNR \_\_\_\_\_  
Design File Location(s) \_\_\_\_\_

2. DESIGN CHECK

Type of Check	Signature(s)	Comments: (Including Reference to Check Document If Appropriate)
A. No check considered necessary	_____	_____
B. Check vs. previous results/issues	_____	_____
C. Checked calculations made	_____	_____
D. Checked computer input and/or output	_____	_____
E. Computer Programs approved/qualified	_____	_____
F. Performed independent audit	_____	_____
G. Spot checked significant points	_____	_____
H. Reviewed methods used	_____	_____
I. Reviewed results for reasonableness	<u>STL</u>	_____
J. Comparison with test data	_____	_____
K. Reviewed vs. drawings	_____	_____
L. Verified procedures	_____	_____
M. Technical content reviewed	_____	_____
N. Management verification of adequate review by others	_____	_____
O. Performed Lessons Learned Search	_____	_____
P. Used Measurement Uncertainty Methods	_____	_____
Q. Other Checks (Describe)	_____	_____

3. CONCURRENCE REQUIREMENTS:

ARP MANAGER  
NUCLEAR ENGINEERING  
REACTOR TH/MECH DESIGN  
REACTOR EQUIPMENT  
POWER PLANT MECHANICAL  
POWER PLANT ELECTRICAL  
FINANCE  
NEW SHIP PROGRAMS  
PROGRAM COORDINATION

Indicate signatures required by X:

NCSG	FLUID DYNAM
ADVANCED CONCEPTS	STRUC. ENGRG
NOISE & ELEC. TECH.	DRAFTING
SHIELDING	QA
REACTOR SAFETY	OTHER
TO	BETTIS
RSO	BPMI
FSO	ADMIN REVIEW
MDO	<u>CR</u>

Cognizant Manager Lynn E. Kolbyra Manager, MDO/SMU/1-44D  
(Must Be Subsection or Higher for External Letters)

4. AUTHORIZED CLASSIFIER: Reviewed By: Lynn E. Kolbyra CLASSIFICATION: Unclassified

5. RELATED SUBJECTS: Commitment Made (Y/N) N Commitment Complete (Y/N) N  
UTRS Implication (Y/N) N UTRS Doc. # \_\_\_\_\_  
Safety Council Review (Y/N) N

6. Distribution:

**6. Distribution:**

**NR**

D.I. Curtis (for info)  
J. D. Yoxtheimer  
J.P. Mosquera  
S.T. Bell  
C.H. Oosterman  
T.N. Rodeheaver

W. Rafaniello  
R.A. Mulford(\*)  
C. Jordan(\*)  
S. Ricca(\*)  
J. Beale(\*)  
L.E. Kolaya  
Y.. Ballout

**PNR**

J.F. Koury  
J.A. Andes

B.C. Campbell  
G.A. Newsome  
T. Schafer(\*)  
J.M. Ashcroft(\*)  
K.C. Loomis(\*)

**SNR**

H. Miller  
D. Potts  
D. Clapper  
G.M. Millis

D. McCoy(\*)  
C. Dempsey(\*)  
H. Schwartzman(\*)  
J.W. Prybylowski  
J.K. Witter(\*)  
M. Wollman

**BETTIS**

R. W. Smith  
S. D. Harkness (\*)  
J.E. Hack  
R. Baranwal  
D.C. Noe(\*)  
C.D. Eshelman  
W.L. Ohlinger(\*)  
M.J. Zika

J.N. Ferrucci(\*)  
K.L. Cotterell(\*)  
S. Samuell(\*)  
W. Gideon(\*)  
SM File  
ADSARS

**KAPL**

S.A. Simonson  
J. Fish(\*)  
S. Gabris(\*)  
R.J. Grossman(\*)

(\*) Electronic mail only